ELSEVIER

NeuroImage

www.elsevier.com/locate/ynimg
NeuroImage 35 (2007) 1365–1377

The roles of prefrontal and posterior parietal cortex in algebra problem solving: A case of using cognitive modeling to inform neuroimaging data

Jared F. Danker* and John R. Anderson

Department of Psychology and Center for the Neural Basis of Cognition, Carnegie Mellon University, Pittsburgh, PA 15213, USA

Received 1 November 2006; revised 17 January 2007; accepted 19 January 2007
Available online 13 February 2007

In naturalistic algebra problem solving, the cognitive processes of representation and retrieval are typically confounded, in that transformations of the equations typically require retrieval of mathematical facts. Previous work using cognitive modeling has associated activity in the prefrontal cortex with the retrieval demands of algebra problems and activity in the posterior parietal cortex with the transformational demands of algebra problems, but these regions tend to behave similarly in response to task manipulations (Anderson, J.R., Qin, Y., Sohn, M.-H., Stenger, V.A., Carter, C.S., 2003. An information-processing model of the BOLD response in symbol manipulation tasks. *Psychon. Bull. Rev.* 10, 241–261; Qin, Y., Carter, C.S., Silk, E.M., Stenger, A., Fissell, K., Goode, A., Anderson, J.R., 2004. The change of brain activation patterns as children learn algebra equation solving. *Proc. Natl. Acad. Sci.* 101, 5686–5691). With this study we attempt to isolate activity in these two regions by using a multi-step algebra task in which transformation (parietal) is manipulated in the first step and retrieval (prefrontal) is manipulated in the second step. Counter to our initial predictions, both brain regions were differentially active during both steps. We designed two cognitive models, one encompassing our initial assumptions and one in which both processes were engaged during both steps. The first model provided a poor fit to the behavioral and neural data, while the second model fit both well. This simultaneously emphasizes the strong relationship between retrieval and representation in mathematical reasoning and demonstrates that cognitive modeling can serve as a useful tool for understanding task manipulations in neuroimaging experiments.

The essence of mathematical problem solving is to call on mathematical knowledge to re-represent problems in a way that moves towards solutions. The NCTM standards (2000) for mathematics education recognize effective use of problem representation as a key educational goal. The interaction between knowledge and representation is particularly apparent in the solution of algebra equations, in which knowledge is brought to bear via the retrieval of mathematical facts and representation is brought to bear via transformations of the problem state. For instance, consider the model developed by Anderson et al. (1996) for solving equations like $x/3+2=8$. The model retrieved the difference $8-2=6$, then transformed the equation to $x/3=6$, then retrieved the multiplication fact $3*6=18$, and finally transformed the equation to $x=18$. Anderson et al. (2003) followed up on the Anderson et al. (1996) behavioral study with an fMRI imaging study to find the neural correlates of retrieval and transformation. That study found evidence that retrieval is supported by a prefrontal region and transformation by a posterior parietal region. This initial conclusion has been supported by a number of subsequent studies with real and artificial algebraic materials (Qin et al., 2003, 2004; Anderson, in press). These subsequent studies all used the same predefined prefrontal and parietal regions.

The association of the prefrontal cortex with memory retrieval and the parietal cortex with representation is generally consistent with the literature. The prefrontal cortex has been repeatedly implicated in imaging research as important for memory in general and retrieval attempts in particular (e.g., Badre and Wagner, 2005; Buckner et al., 1999; Cabeza et al., 2002; Dobbins and Wagner, 2005; Fletcher and Henson, 2001; Köhler et al., 2004; Lepage et al., 2000; Sohn et al., 2003, 2005; Thompson-Schill, 2003; Wagner et al., 2001a,b). These imaging results are consistent with neuropsychological evidence that prefrontal lesions are associated with difficulties in memory retrieval (Stuss and Benson, 1984; Shimamura, 2005). Consistent with its role in mental representation, the parietal cortex has been implicated in verbal encoding (Clark and Wagner, 2003; Davachi et al., 2001), mental rotation (Alivisatos and Petrides, 1997; Carpenter et al., 1999; Heil, 2002; Richter et al., 1997; Zacks et al., 2002), and visuospatial strategies in linguistic (Reichle et al., 2000) and mathematical (Dehaene et al., 1999; Sohn et al., 2004) contexts. While the parietal cortex is often active in memory tasks, a number of theorists have proposed

* Corresponding author. Fax: +1 412 268 2798.
E-mail address: jdanker@andrew.cmu.edu (J.F. Danker).
Available online on ScienceDirect (www.sciencedirect.com).

1053-8119/$ - see front matter © 2007 Elsevier Inc. All rights reserved.
doi:10.1016/j.neuroimage.2007.01.032

that it serves a support role, such as in the strategic use of mental imagery (Fletcher et al., 1995; Rugg and Henson, 2002) or in working memory maintenance (Wagner et al., 2005). This kind of suggestion is supported by recent evidence showing that magnetic stimulation of the posterior parietal cortex interferes with performance in visuospatial processing, but not memory retrieval (Rossi et al., 2006), whereas similar stimulation to the prefrontal region does impair memory retrieval (Rossi et al., 2001).

The goal of the current research is to further develop the role of these two regions in equation solving by isolating the processes of transformation and retrieval in time. This will enable better identification of the fMRI activity reflecting these two cognitive processes. We will test our understanding of these processes by modeling the data within an information-processing theory called the adaptive control of thought—rational (ACT-R; Anderson et al., 2004). We have mapped components or modules in ACT-R onto the different regions of the brain (Anderson, 2005). Of particular relevance to the current discussion, a retrieval module responsible for the retrieval of declarative memories has been associated with the prefrontal region and an imaginal module responsible for the transformation and manipulation of mental representations has been associated with the parietal region. In the context of mentally solving algebra problems, the retrieval module is responsible for the retrieval of arithmetic facts (e.g., $8-2=6$), and the imaginal module is responsible for encoding and transforming representations of the problem (e.g., from $x/3+2=8$ to $x/3=6$).

In normal equation solving, the retrieval of arithmetic facts and the transformation of the equation occur in quick succession. For this reason, our previous studies of equation solving have shown (and predicted) highly correlated activity in prefrontal and parietal regions (Anderson et al., 2003; Qin et al., 2003, 2004; Anderson, in press). In the experiment to be reported here we attempt to isolate activity in these two regions by using a multi-step algebra task in which transformation is manipulated in the first step and retrieval is manipulated in the second step. These steps are either separated by an 8-s delay or not. Fig. 1 illustrates the basic structure of the experiment. We will manipulate both the difficulty of the transformation step and the difficulty of the retrieval step. In the condition where these two steps are separated by 8 s we will get a fairly clear picture of their effect on the prefrontal and parietal regions. The immediate condition will allow us to determine whether this 8-s delay had in any way changed the fundamental processes. We will attempt to develop a model that can account for the latency effects in the data and check the predictions of that model for the parietal and prefrontal regions. We have suggested that the interaction between retrieval and representation is integral to mathematical thinking. By combining cognitive modeling with neuroimaging data, we hope to shed some light on whether these processes can be separated in a mathematical context.

Method

Participants

The participants were 20 right-handed English speakers (nine females, ages 20 to 53, mean age 25). Institutional review board approval was obtained from both Carnegie Mellon University and the University of Pittsburgh. All participants were given informed consent in accordance with Carnegie Mellon University and University of Pittsburgh guidelines.

Stimuli

Thirty-two algebra equations (see Appendix A) were created that could be simplified to the *x*-isolated form *x=a operator b* in one step. The *x*-isolated form could be $x=a+b$, $x=a-b$, $x=a*b$, or $x=a/b$. In any given equation, *x* could be isolated by adding, subtracting, multiplying, or dividing either *a* or *b* on both sides of the equation, resulting in eight different simplification operations. Combining all possible combinations of *x*-isolated forms and simplification operations yields 32 algebra equations. These equations, which require one step to solve, are *high transformation* equations. For each high transformation equation, a corresponding *low transformation* equation was created that was already in the *x*-isolated form *x=a operator b*, but had identity operations such as 1*, /1, +0, and −0 inserted such that the two equations had an equal number of visual characters. Relative to the low transformation equations, the high transformation equations required an extra transformation corresponding to the simplification operation. The 32 high transformation equations and their matched low transformation equations are presented in Appendix A.

Numerical values of *a* and *b* were randomly created separately for each participant such that the value of *x* once the equation was solved always had a 2, 4, 6, or 8 as the ones digit. The values of *a* and *b* were presented in one of two forms. In the *high retrieval*

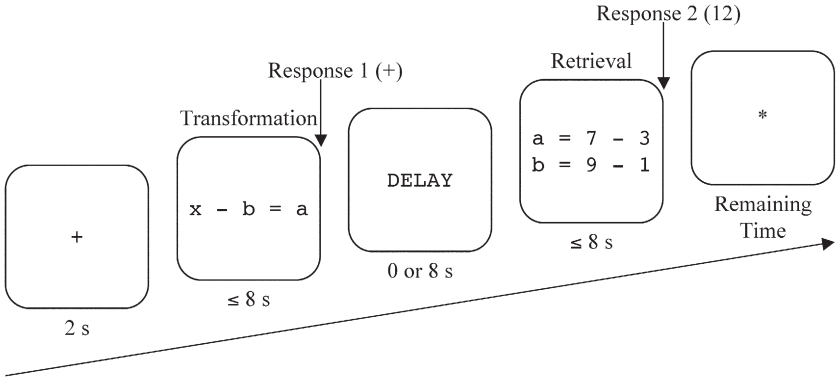

Fig. 1. The timing and structure of an experimental trial.

form, subtractions needed to be performed to get the values of *a* and *b*. In the *low retrieval* form, no subtraction needed to be performed but the identity expression −0 was presented next to the values of *a* and *b* to match on the number of visual characters. Relative to the low retrieval forms, the high retrieval forms required two extra retrievals of arithmetic facts corresponding to the two subtractions. Each of the 64 equations appeared once paired with a high retrieval form of *a* and *b* and once paired with a low retrieval form of *a* and *b*, resulting in 128 unique equation sets per participant. Examples of equation sets in each of the transformation and retrieval conditions are presented in Table 1.

Procedure

The participants solved algebra problems in two stages, as illustrated in Fig. 1. In the first stage (the *transformation stage*), participants were asked to isolate the variable *x* in a high or low transformation equation. Having *a* and *b* in place of actual numbers in these equations allowed participants to isolate *x*, but prevented them from retrieving any arithmetic facts. After they had isolated *x* (in high transformation equations) or recognized that it was already isolated (in low transformation equations), participants were instructed to indicate with a response glove on their right hand whether the operator between *a* and *b* in the *x*-isolated form was addition (index finger), subtraction (middle finger), multiplication (ring finger), or division (little finger). This response ensured that participants had simplified the equation into an *x*-isolated form before moving on to the next stage of the problem. The mapping of fingers to responses was presented on screen.

After participants responded, there was either an 8-s delay or not. During the delay period, participants were instructed to remember their response from the transformation stage (i.e., the *x*-isolated form of the equation). After the delay period, the numerical values of *a* and *b* were presented on screen such that participants could calculate *x* either by immediately plugging the values of *a* and *b* into the *x*-isolated form (low retrieval form) or by doing so after calculating the values of *a* and *b* individually by subtraction (high retrieval form). This is called the retrieval stage. Participants were instructed to indicate the ones digit of the value of *x* (i.e., 2 for 2, 12, 22, etc.), which was 2 (index finger), 4 (middle finger), 6 (ring finger) or 8 (little finger). Again, this mapping of fingers to responses was presented on screen.

Each stage ended either when the participant responded or after 8 s had passed (in which case the response was coded as incorrect). After their response to the retrieval stage, the information on screen was replaced with an asterisk (*) until the trial had lasted 18 s (no-delay trials) or 26 s (delay trials). Finally, a plus sign (+) appeared for 2 s to indicate that the next trial was about to begin.

Table 1
Example stimuli for high and low transformation and retrieval trials

	Low transformation	High transformation
Low retrieval	Equation: $x=a+b$ Values: $a=4-0$; $b=8-0$	Equation: $x-b=a$ Values: $a=4-0$; $b=8-0$
High retrieval	Equation: $x=a+b$ Values: $a=7-3$; $b=9-1$	Equation: $x-b=a$ Values: $a=7-3$; $b=9-1$

Design

The three major factors of interest were transformation, retrieval, and delay, resulting in 8 conditions. There were 128 trials total and 16 trials per condition. There were 8 blocks per participant and 16 trials per block. Within each block, there were two trials for each of the 8 cells such that there were an equal number of delay and no-delay trials in any given block (thus equating the blocks on length). Participants received feedback in the form of percent correct values at the end of each block. Trials were presented in random order within and between blocks.

fMRI procedure

Event-related fMRI data were collected using a gradient echo-planar-image (EPI) acquisition on a Siemens 3 T Allegra Scanner. The imaging parameters were TR=2000 ms, TE=30 ms, flip angle=79°, FOV=200 mm, matrix size=64×64, slice thickness=3.2 mm, slice gap=0 mm, and 34 axial slices per scan with AC–PC on the 11th slice from the bottom. There were 10 scans for each no-delay trial and 14 scans for each delay trial.

Anatomical scans were acquired by using a standard T2-weighted pulse sequence, with 34 slices and the AC–PC on the 11th slice from the bottom. Images were coregistered to a common reference anatomical MRI scan by means of the 12-parameter AIR algorithm (Woods et al., 1998) and smoothed with a 6-mm full-width half-maximum three-dimensional Gaussian filter. When the anatomical images were being collected, participants performed two blocks of practice trials. The first block gave feedback after each response, while the second block gave feedback only at the end of the block.

Results

Behavioral

The mean latencies of the responses to the transformation and retrieval stages of the trial are displayed in Figs. 2A and B, respectively. The dashed and dotted lines are predictions of two models that will be discussed later. The means are calculated using correct trials only, and are pooled across delay and no-delay conditions. Separate 2-transformation×2-retrieval×2-delay repeated-measures ANOVAs were performed on the transformation and retrieval stages. In the transformation stage (Fig. 2A), response times were significantly longer for high transformation trials than low transformation trials (abscissa, $F(1,19)=314$, MSE=118987, $p<0.01$), but response times were not different for low and high retrieval trials (symbols, $F(1,19)=0$, MSE=42892, $p>0.10$). Correspondingly, during the retrieval stage (Fig. 2B), response times were significantly longer for high retrieval trials than low retrieval trials (abscissa, $F(1,19)=1226$, MSE=183747, $p<0.01$), but there was no difference between high and low transformation trials (symbols, $F(1,19)=2.62$, MSE=87222, $p>0.10$). There was also a small effect of delay on the retrieval stage ($F(1,19)=6.48$, MSE=198660, $p<0.05$) such that participants were slower by 180 ms when there was a

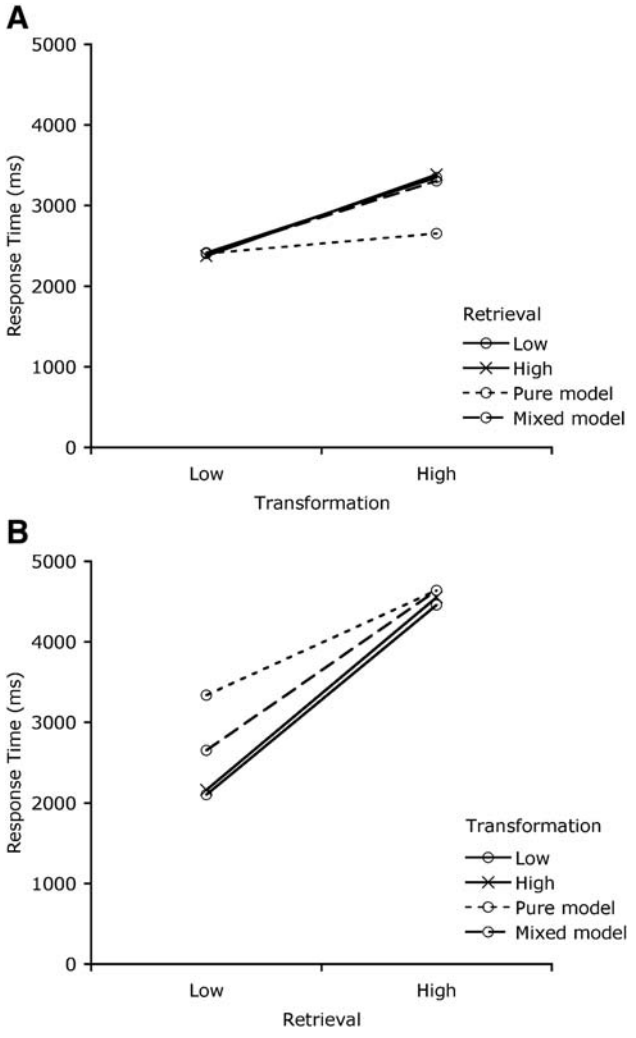

Fig. 2. The mean response latencies and model predictions in the transformation (A) and retrieval (B) stages.

delay. These results suggest that the manipulations had their intended effects and that there were no carryover effects across stages.

There is a strong negative correlation between latency and accuracy ($r=-0.899$ for transformation and $r=-0.963$ for retrieval). The same 2-transformation × 2-retrieval × 2-delay repeated-measures ANOVAs were performed separately on transformation and retrieval stages with accuracy as the dependent measure. In the transformation stage, accuracy was significantly lower for high transformation than low transformation trials ($F(1,19)=8.52$, MSE=0.019, $p<0.01$), but accuracy was not different for high and low retrieval trials ($F(1,19)=1.47$, MSE=0.019, $p>0.10$). Correspondingly, in the retrieval stage, accuracy was significantly lower for high retrieval trials than low retrieval trials ($F(1,19)=60.93$, MSE=0.014, $p<0.01$), but there was no difference between low and high transformation trials ($F(1,19)=2.62$, MSE=0.007, $p>0.10$), and no effect of delay ($F(1,19)=1.82$, MSE=0.007, $p>0.10$). Overall, these results confirm that high transformation and high retrieval trials were more difficult than low transformation and low retrieval trials, respectively, in terms of both response time and accuracy.

Imaging: predefined regions

We used the same predefined parietal and prefrontal regions that have been used in previous studies by our group (Anderson et al., 2003; Qin et al., 2003, 2004). Both are 5 voxels wide, 5 voxels long, and 4 voxels deep. The parietal region was centered at Talairach coordinates $x=-23$, $y=-64$, $z=34$. This includes parts of Brodmann areas 7, 39, and 40 at the border of the intraparietal sulcus. The prefrontal region was centered at Talairach coordinates $x=-40$, $y=21$, $z=21$. This includes parts of Brodmann areas 45 and 46 around the inferior frontal sulcus. All analyses on imaging data were performed on correct trials only. In addition, trials with scan-to-scan fluctuations in the BOLD signal exceeding 5% were excluded from analyses.

Figs. 3 and 4 display the BOLD responses for the left parietal and prefrontal regions where the dependent measure is calculated as the percent BOLD signal change in the region of interest, relative to a baseline on scans 1 and 2. Solid lines correspond to the data, while dotted lines correspond to model predictions and can be ignored for the time being. For each predefined region, a 2-transformation × 2-retrieval × 10-scan repeated-measures ANOVA was performed for the no-delay trials and a 2-transformation × 2-retrieval × 14-scan repeated-measures ANOVA was performed for the delay trials. To deal with the non-independence of scans we treat the F-values for these interactions with scan as having 1 degree of freedom in their numerator (the lower bound correction).

The parietal region showed effects both in line with and in contrast with our predictions. In all cases, the more difficult conditions (high retrieval and high transformation) were associated with more neural activity (Fig. 3). In the delay condition, it showed significant effects of both retrieval ($F(1,19)=3.38$, MSE=0.08, $p<0.10$ for main effect; $F(1,19)=9.52$, MSE=0.02, $p<0.01$ for interaction) and transformation ($F(1,19)=1.67$, MSE=0.24, $p>0.10$ for main effect; $F(1,19)=10.03$, MSE=0.01, $p<0.01$ for interaction). In the no-delay condition it showed an effect of retrieval ($F(1,19)=25.86$, MSE=0.09, $p<0.0001$ for main effect; $F(1,19)=20.55$, MSE=0.01, $p<0.01$ for interaction) but not transformation ($F(1,19)=0.48$, MSE=0.17, $p>0.10$ for main effect; $F(1,19)=0.88$, MSE=0.01, $p>0.10$ for interaction).

In order to better characterize the interactions in the delay condition, a 2-transformation × 2-retrieval × 2-stage repeated-measures ANOVA was performed on the parietal region. The dependent measure was the BOLD response averaged across scans 4–7 after the start of the transformation or retrieval stage. Significant interactions between transformation and stage ($F(1,19)=25.21$, MSE=0.16, $p<0.01$) as well as retrieval and stage ($F(1,19)=40.86$, MSE=0.26, $p<0.01$) indicate that both manipulations had stronger effects during the appropriate stage of the trial. It can be seen from this analysis that the delay manipulation allowed us to better characterize effects that were difficult to characterize or entirely absent in the no-delay condition. Inserting a delay allowed us to see that, counter to our predictions, the parietal region actually responded to both the transformation and retrieval manipulations at appropriate times during the trial.

The prefrontal region showed the expected effects of retrieval. Across the no-delay (Fig. 4C) and delay (Fig. 4D) conditions, there was a more positive-going BOLD response in the prefrontal cortex in the high retrieval condition than in the low retrieval condition. In the delay condition, the main effect of retrieval was not significant ($F(1,19)=1.89$, MSE=0.09, $p>0.10$), but the interaction with scan

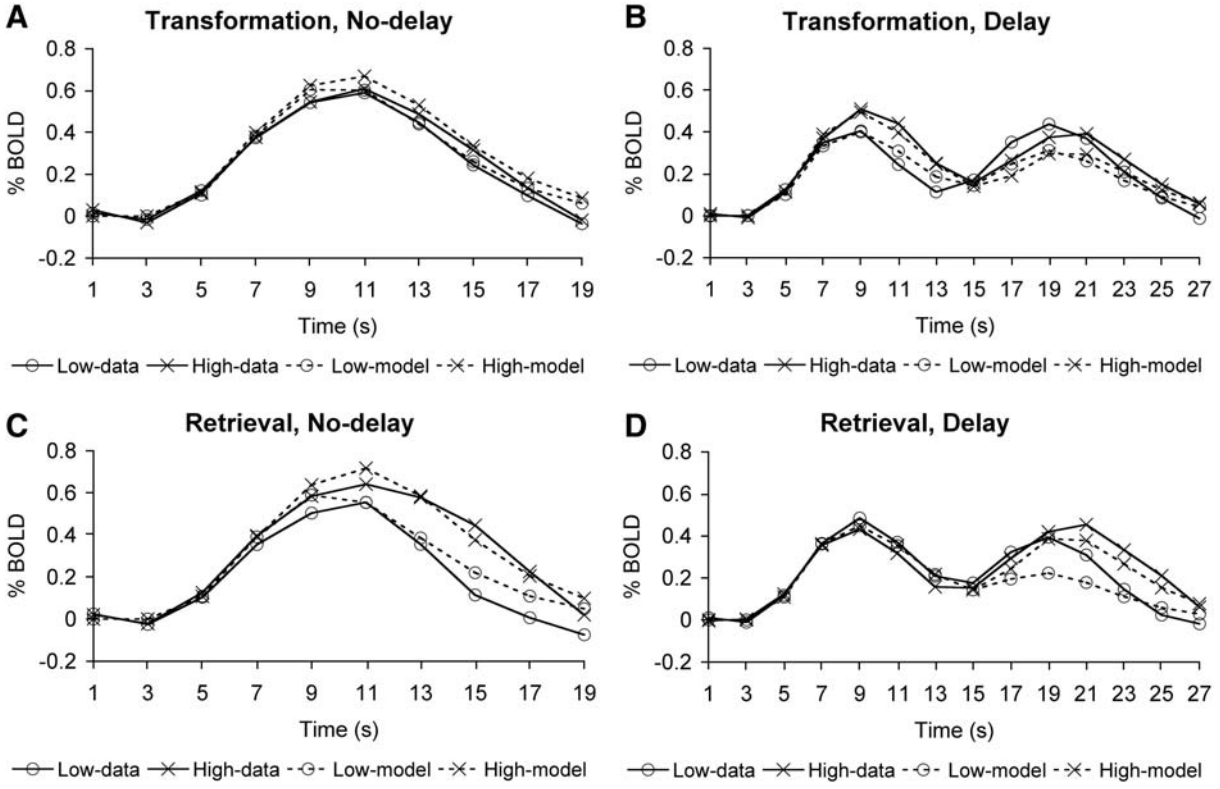

Fig. 3. The BOLD response and model predictions in the left posterior parietal cortex for the effects of transformation in the no-delay (A) and delay (B) conditions as well as the effects of retrieval in the no-delay (C) and delay (D) conditions.

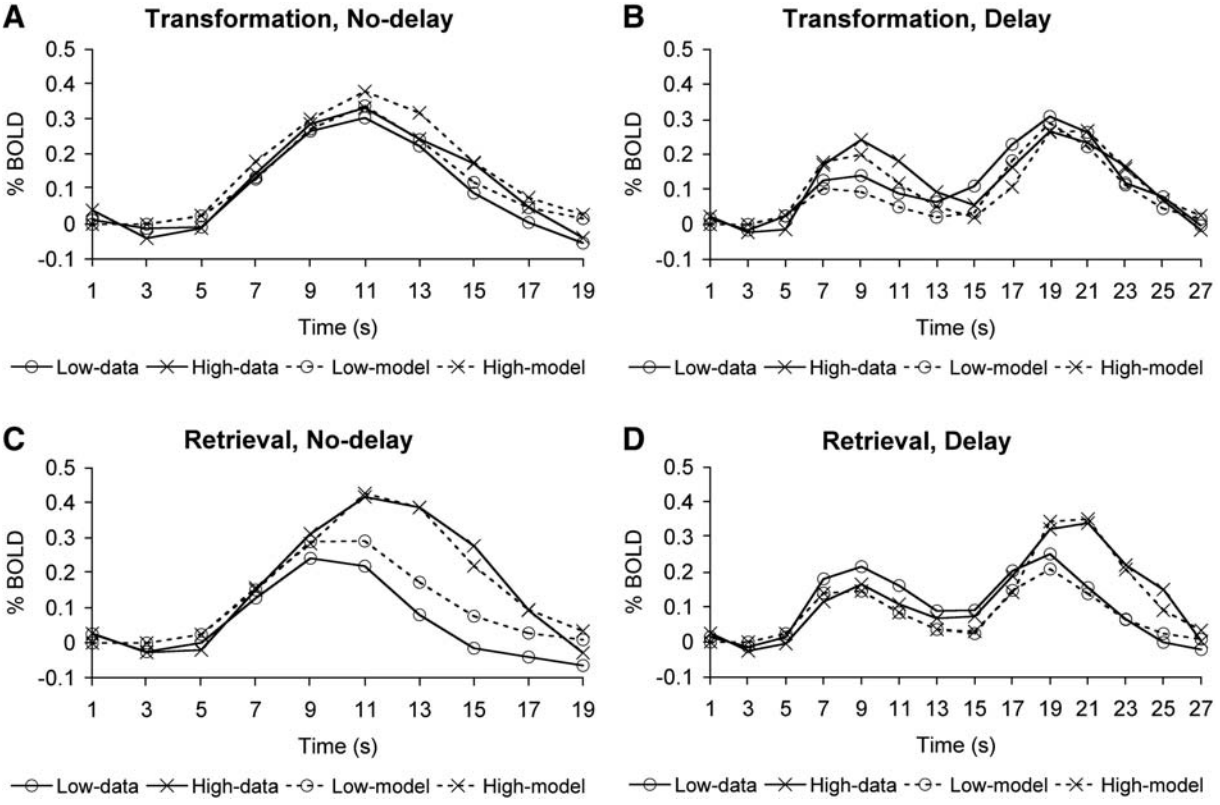

Fig. 4. The BOLD response and model predictions in the left prefrontal cortex for the effects of transformation in the no-delay (A) and delay (B) conditions as well as the effects of retrieval in the no-delay (C) and delay (D) conditions.

was significant ($F(1,19)=7.13$, MSE=0.02, $p<0.05$). In the no-delay condition both effects were significant ($F(1,19)=30.22$, MSE=0.08, $p<0.01$ for main effect; $F(1,19)=18.85$, MSE=0.02, $p<0.0005$ for interaction). There appeared to be a stronger BOLD response in the high transformation condition than the low transformation condition across no-delay (Fig. 4A) and delay (Fig. 4B) trials, but none of the effects associated with transformation were significant either in the delay condition ($F(1,19)=0.10$, MSE=0.18, $p>0.10$ for main effect; $F(1,19)=3.86$, MSE=0.18, $p<0.10$ for interaction) or in the no-delay condition ($F(1,19)=0.73$, MSE=0.14, $p>0.10$ for main effect; $F(1,19)=1.07$, MSE=0.02, $p>0.10$ for interaction).

In order to better investigate the effects of retrieval and transformation during the delay condition, a 2-transformation × 2-retrieval × 2-stage repeated-measures ANOVA was performed on the prefrontal region. This is the same focused analysis that we used for the parietal region. Significant interactions between retrieval and stage ($F(1,19)=35.60$, MSE=0.35, $p<0.01$) as well as transformation and stage ($F(1,19)=11.74$, MSE=0.08, $p<0.01$) indicate that the prefrontal cortex actually responded to both manipulations during their appropriate stages. Again, inserting a delay allowed us to better characterize the response characteristics of a region to our task manipulations. In this case, it allowed us to see that the prefrontal region actually responded to the transformation manipulation as well as the retrieval manipulation.

Finally, we performed a 2-region × 2-stage × 2-transformation × 2-retrieval repeated-measures ANOVA on the delay condition. The dependent measure was the percent BOLD signal change averaged across scans 4–7 after the start of the transformation or retrieval stage of the trial. In this ANOVA, a significant region × transformation interaction could indicate that the parietal region responded more strongly to the transformation manipulation, and a significant region × retrieval interaction could indicate that the prefrontal cortex responded more strongly to the retrieval manipulation. In addition, a significant region × stage × transformation or region × stage × retrieval interaction could indicate that these effects were dependent on the stage in the trial. However, there were no significant region × transformation ($F(1,19)=1.94$, MSE=0.02, $p>0.10$) or region × retrieval ($F(1,19)=0.08$, MSE=0.0007, $p>0.10$) interactions, and there were also no region × stage × transformation ($F(1,19)=1.57$, MSE=0.005, $p>0.10$) or region × stage × retrieval ($F(1,19)=0.59$, MSE=0.003, $p>0.10$) interactions. This indicates that neither of the two regions responded significantly differently to the two manipulations, with parietal and prefrontal regions responding similarly to increases in transformation or retrieval difficulty.

Imaging: exploratory regions

In this section, the results of the exploratory analyses will be reported. ROIs were selected that showed significant condition (4 conditions defined by the cross of transformation and retrieval) × scan interactions, and consisted of at least 10 contiguous voxels at $p<0.001$ (no-delay) or $p<0.005$ (delay). The lower bound correction was applied to the interaction terms. The resulting regions are displayed in Fig. 5 and listed in Table 2 along with their sizes and locations. Regions with significant interactions showed effects of transformation or retrieval that were dependent on scan (i.e., an effect that changes over time), and most of them could be characterized as having a differential rise in the percent BOLD change across conditions relative to baseline (scans 1 and 2). Thus, Table 2 reports the *t* values associated with the difference in average percent BOLD change between the low and high conditions. There are separate *t* values reported for the effects of transformation and retrieval. Positive *t* values indicate that the region responded more positively in the high condition and negative *t* values indicate that the region responded more positively in the low condition. All regions demonstrating negative *t* values also showed negative task-related activity. The average percent BOLD change was calculated as the average BOLD change across scans 3–10 in the no-delay condition and across scans 3–14 in the delay condition (scans 1 and 2 are baseline).

Table 2A and Fig. 5A show the 11 regions showing significant condition × scan interactions in the no-delay condition. All of these regions responded more strongly to the retrieval manipulation than the transformation manipulation, which is consistent with the large difference in behavioral effect sizes between the two manipulations (see Fig. 2). Included in these regions are areas overlapping with our predefined parietal (c, green) and prefrontal (d, yellow) regions. The *t* values show that these regions responded to increased transformation and retrieval demands with increased activity, but only the retrieval effects were significant. In addition to these regions, parts of the left precentral gyrus (a, red), anterior cingulate (b, blue), bilateral insula (h, indigo), and occipital cortex (i, white) responded with increased activity to higher transformation and retrieval demands. In contrast, the polar frontal cortex (e, pink), bilateral angular gyrus (f, purple), and precuneus (g, orange) responded more negatively to higher transformation and retrieval demands. Table 2B and Fig. 5B show the eight regions that demonstrate significant condition × scan interactions in the delay condition. All of these regions were significant in the no-delay condition as well.

Modeling

Having now reviewed the results of the experiment, we come to the question of whether we can understand them in the framework of the ACT-R theory (Anderson et al., 2004). The ACT-R theory is instantiated as a series of central and perceptual–motor modules driven by a production system. The production system reads information in each of the modules and chooses the appropriate action based on a series of learned condition–action pairings (productions), a process modeled as taking 50 ms. The imaginal and retrieval modules are the most pertinent to the current discussion. The imaginal module is responsible for encoding and transforming problem representations and has been associated with the parietal cortex. An imaginal operation in ACT-R is modeled as taking 200 ms by default. The retrieval module is responsible for retrieving declarative memories and has been associated with prefrontal cortex. Retrieval time is a free parameter in ACT-R. The methodology is to find an ACT-R model that can account for the latency pattern observed and then

Fig. 5. Predefined and exploratory regions across no-delay (A) and delay (B) conditions. Predefined prefrontal and posterior parietal regions are shown in black; exploratory regions are in color and are: (a) precentral gyrus—red, (b) anterior cingulate—blue, (c) parietal lobule—green, (d) middle frontal gyrus—yellow, (e) polar—frontal pink, (f) angular gyrus—purple, (g) precuneus—orange, (h) insula—indigo, (i) occipital—white.

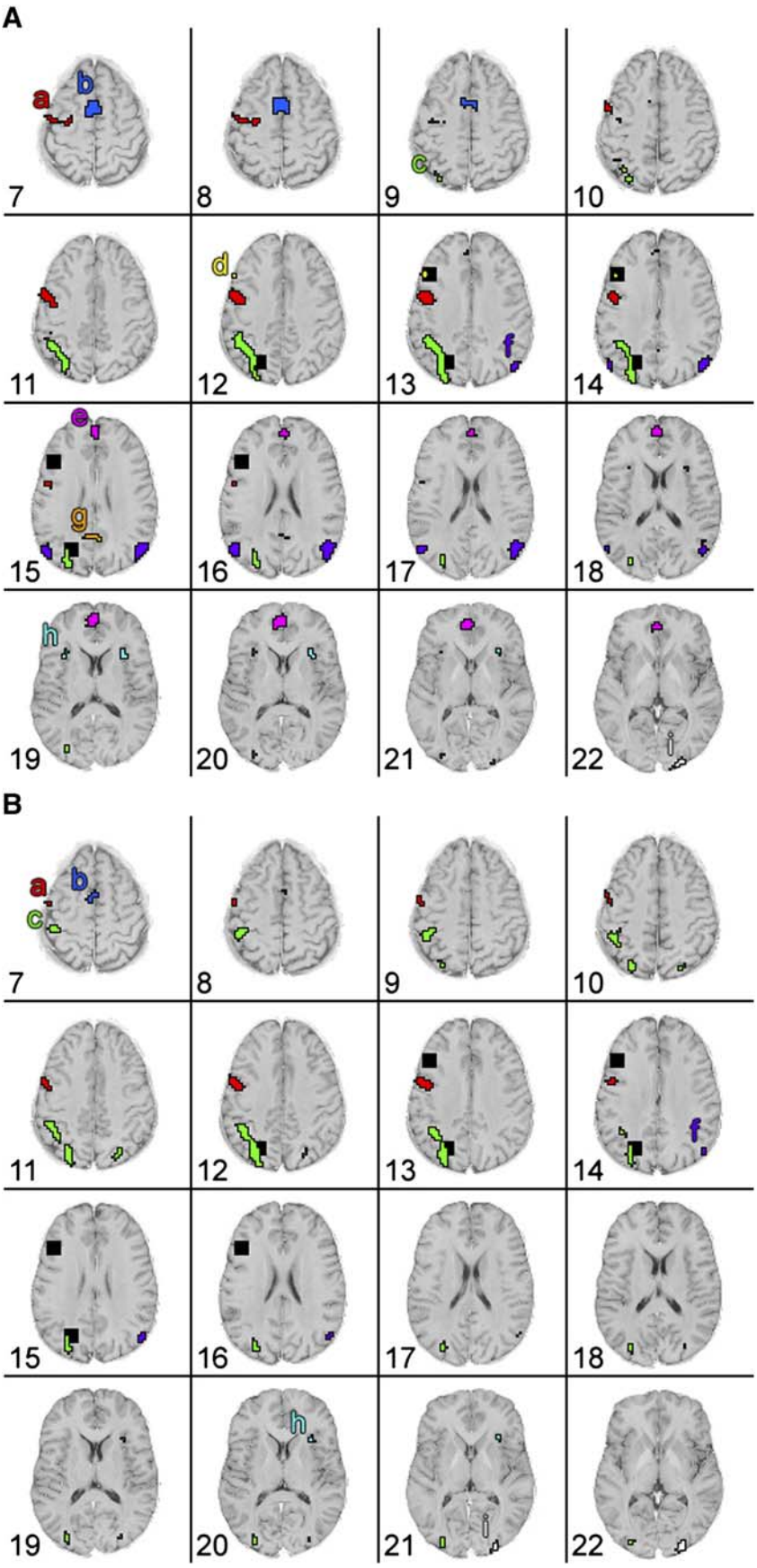
A
a
b
7
8
c
9
10
11
d
12
f
13
14
e
g
15
16
17
18
h
19
20
21
i
22
B
a
b
c
7
8
9
10
11
12
13
f
14
15
16
17
18
h
19
20
i
21
22

Table 2
Results of exploratory analyses — see Fig. 4

Region of interest	Brodmann area(s)	Voxel count	Coordinates			*t* Value transform	*t* Value retrieval
			x	*y*	*z*		
A. No-delay condition							
a. L. precentral gyrus	6	185	−46	0	36	2.10[a]	7.50[b]
b. Anterior cingulate	6, 32	121	0	5	50	1.66	5.89[b]
c. L. parietal lobule	7, 39, 40	293	−30	−56	42	1.89[c]	8.59[b]
d. L. middle frontal	9, 46	17	−46	25	28	1.52	5.75[b]
e. Polar frontal	10, 32	124	0	50	5	−1.49	−5.09[b]
f. R. angular gyrus	39	120	50	−65	35	−0.66	−7.18[b]
f. L. angular gyrus	39	59	−50	−65	35	−0.38	−4.57[b]
g. Precuneus	7. 31	19	0	−50	30	−1.75[c]	−3.72[b]
h. R. insula	13	27	30	17	7	1.44	5.37[b]
h. L. insula	13	13	−30	17	7	2.26[a]	6.90[b]
i. Occipital	17, 18	727	0	−77	−10	2.15[a]	5.65[b]
B. Delay condition							
a. L. precentral gyrus	6	99	−46	0	36	0.79	3.14[b]
b. Anterior cingulate	6, 32	28	0	5	50	1.55	3.25[b]
c. R. parietal lobule	7	22	26	−68	48	2.30[a]	1.11
c. L. parietal lobule	7, 39, 40	374	−30	−56	42	1.95[c]	1.65
f. R. angular gyrus	39	25	50	−65	35	−2.47[a]	−3.35[b]
h. R. insula	13	14	30	17	7	1.75[c]	2.53[a]
i. R. occipital	17–19	408	35	−77	10	1.64	3.09[b]
i. L. Occipital	17–19	116	−35	−77	10	3.01[b]	3.44[b]

[a] $p<0.05$.
[b] $p<0.01$.
[c] $p<0.10$.

see whether it can predict the pattern of observations in the parietal and prefrontal regions. In advance of doing the experiment we had a model in mind that we call the pure manipulation model in which the transformation stage of the experiment only manipulated imaginal operations and the retrieval stage of the experiment only manipulated retrieval operations. This model was less than successful in predicting the latency data and therefore we developed a slightly more complex model that we call the mixed manipulation model. Below we will describe the two models and their fit to the latency data, and then we will describe a fit of the mixed manipulation model to the BOLD response in the parietal and prefrontal regions. These models were strongly influenced by the algebra problem solving model of Anderson et al. (1996). All model parameters were set to ACT-R's default values, with the exception of the retrieval duration parameter, which was set to 600 ms to be consistent with the previous model (Anderson et al., 1996).

Pure manipulation model

A simplified version of how the pure manipulation model solves problems in each of the four combinations of transformation and retrieval conditions is presented in Fig. 6A for the examples shown in Table 1. This is the model for the no-delay condition but we assume the delay condition is achieved by adding 8 s of inactivity between the transformation and retrieval stages (after the first response). In Fig. 6, the imaginal module would be responsible for "encode" and "transform" operations (light grey), and the retrieval module would be responsible for "retrieve" operations (dark grey). The details of the model are simplified for display purposes.[1] Specifically, the underlying productions driving the retrieval and imaginal modules are not shown. The pure manipulation model responds to the transformation manipulation by performing one extra transformation (e.g., simplifying $x-b=a$ to $x=a+b$) using the imaginal module, but does not perform any extra retrievals. This model responds to the retrieval manipulation by performing two extra retrievals (corresponding to the two subtractions $a=7-3$ and $b=9-1$) using the retrieval module, but does not perform any extra transformations. To put it simply, the pure manipulation model responds to our experimental design as we intended.

The fit of the predictions of the pure manipulation model to the RT data is presented in Fig. 2. Solid lines represent the data, and dotted lines represent the predictions of the pure manipulation model. Only one line is presented in each figure because the model makes identical predictions for the factor represented by the different symbols. During the transformation stage (Fig. 2A), it can be seen that the low transformation condition fits the data rather well, but the high transformation condition underestimates the data. This leads to a predicted effect size (250 ms) that is much smaller than the actual effect size (970 ms). The predicted effect size of the transformation manipulation is comprised of the extra transformation (200 ms) and an additional production (50 ms). During the retrieval stage (Fig. 2B), the high retrieval condition fits rather well, but the low retrieval condition strongly overestimates the data. This likewise leads to a predicted effect size (1300 ms) that is much smaller than the effect size in the data (2370 ms). The

[1] But the actual running ACT-R models are available at http://act-r.psy.cmu.edu/papers/689/models.zip.

predicted effect size of the retrieval manipulation consists of the two extra retrievals (600 ms each) and two additional productions (50 ms each). These two retrievals correspond to the two subtractions performed to obtain the values of *a* and *b* in the high retrieval condition. Overall, this model leads to a rather poor fit of the RT data ($R^2 = 0.50$). This finding suggests that participants may not have performed the task in the same way as the pure manipulation model.

Mixed manipulation model

Because the model implicit to our experimental design (the pure manipulation model) did not fit the RT data well, we attempted to design a model with identical parameters that did fit the data. A simplified example of how this model, which we call the mixed manipulation model, solves problems in each of the four combinations of transformation and retrieval conditions is presented in Fig. 6B. Again, the figure represents the model during the no-delay condition but the delay condition can be modeled by adding 8 s of inactivity between the transformation and retrieval stages (after the first response). The mixed manipulation model had to adopt different responses to the task manipulations in order to accomplish a good fit:

1. The transformation manipulation elicited an additional retrieval performed by the retrieval module as well as an additional transformation performed by the imaginal module. This extra retrieval occurred when the model had to retrieve the opposite of a given operator in order to invert that operator and perform the transformation. In the example shown, the model would have to retrieve the fact that + is the opposite of − in order to know to add *b* to both sides of the equation and achieve the simplified version for $x = a + b$. It should be noted that the Anderson et al. (1996) model did involve retrieval operations for transformations.
2. The retrieval manipulation affected the number of transformations as well as the number of retrievals. There was a reduced need to encode characters in the low retrieval condition. Specifically, if the model already encoded that the value of *a* was some number minus zero, it was guaranteed that the value of *b* was some number minus zero. In this case, an efficient model does not need to encode the second zero because it is perfectly predicted by the first zero, which actually results in fewer imaginal operations in the low retrieval condition.

This model would predict that both our predefined parietal region (associated with the imaginal module) and our predefined prefrontal region (associated with the retrieval module) would respond to both manipulations, which is in agreement with our results.

The fit of the predictions of the mixed manipulation model to the RT data is also presented in Fig. 2. The dashed lines represent the predictions of the mixed manipulation model. In the transformation stage (Fig. 2A), both the low transformation condition and the high transformation condition fit the data well. This leads to a predicted effect size (900 ms) that is highly similar to the observed effect size (970 ms). The predicted effect size for the transformation manipulation consists of the extra transformation (200 ms), the extra retrieval (600 ms), and two additional productions (50 ms each). In the retrieval stage (Fig. 2B), the high retrieval condition fit the data well, and the low retrieval condition slightly overestimated the observed data. This likewise leads to a predicted effect size (1985 ms) that is similar to the actual effect size (2370 ms). The predicted effect size for the retrieval manipulation consists of the two extra retrievals (600 ms each), the two additional imaginal operations (200 ms each), one extra visual operation (85 ms), and 6 additional productions (50 ms each). Overall, the predictions of the mixed manipulation model fit the response time data well ($R^2 = 0.94$).

Modeling the BOLD response

While our mixed model is post hoc, it is possible to check it by using it to predict activity in the BOLD response in our predefined regions. As explained in Anderson (2005), if one assumes that whenever a particular module is engaged (e.g., the imaginal module is active during "encode" and "transform" steps in Fig. 6) it will make an increased metabolic demand, then one can use standard assumptions about the hemodynamic response to predict the BOLD response. This involves convolving an engagement function that has the value of 1 whenever the module is active with a hemodynamic function corresponding to the shape of the BOLD response. The hemodynamic function we have adopted is the standard gamma function, which has been used by several other researchers to represent the BOLD response (Boyton et al., 1996; Cohen, 1997; Dale and Buckner, 1997; Glover, 1999). When a module is engaged it will elicit a BOLD response *t* time units later according to the function:

$$H(t) = m\left(\frac{t}{s}\right)^a e^{-(t/s)},$$

where *m* governs the magnitude, *s* scales the time, and the exponent *a* determines the shape of the BOLD response such that functions with larger values of *a* rise and fall more steeply. The BOLD response accumulates whenever a region is engaged according to the engagement function $f(t)$, thus the cumulative BOLD response in a particular region can be calculated by convolving the engagement function with the BOLD function:

$$B(t) = \int_0^t f(x)H(t-x)dx,$$

We used these principles to predict activity in our predefined parietal and prefrontal regions using engagement functions from the imaginal and retrieval modules of the mixed manipulation model. To reiterate, the imaginal module was engaged during "encode" and "transform" operations in Fig. 6B (light grey), and the retrieval module was engaged during "retrieve" operations (dark grey). The values of *m*, *a*, and *s* were calculated to minimize the degree of mismatch against the noise in the data according to the following Chi-squared statistics:

$$\chi^2 = \frac{\sum_i (\hat{\chi}_i - \overline{\chi}_i)^2}{S^2_{\overline{\chi}}},$$

where the denominator is estimated from the interaction term between condition and participants. The best fitting predictions (dotted lines) are displayed along with the data (solid lines) in

A

Scan	Time	Low Transformation		High Transformation	
		Low Retrieval	High Retrieval	Low Retrieval	High Retrieval
1	0.00				
	0.25	Encode x	Encode x	Encode x	Encode x
	0.50	Encode =	Encode =	Encode -	Encode -
	0.75	Encode a	Encode a	Encode b	Encode b
	1.00	Encode +	Encode +	Encode =	Encode =
	1.25	Encode b	Encode b	Encode a	Encode a
	1.50			Transform	Transform
	1.75	Retrieve Key	Retrieve Key		
2	2.00			Retrieve Key	Retrieve Key
	2.25	Respond +	Respond +		
	2.50			Respond +	Respond +
	2.75	Encode 4	Encode 7		
	3.00	Encode 0	Encode 3	Encode 4	Encode 7
	3.25	Encode 8		Encode 0	Encode 3
	3.50	Encode 0	Retrieve 7-3	Encode 8	
	3.75			Encode 0	Retrieve 7-3
3	4.00	Retrieve 4+8	Encode 9		
	4.25		Encode 1	Retrieve 4+8	Encode 9
	4.50				Encode 1
	4.75	Retrieve Key	Retrieve 9-1		
	5.00			Retrieve Key	Retrieve 9-1
	5.25	Respond 2			
	5.50		Retrieve 4+8	Respond 2	
	5.75				Retrieve 4+8
	6.00				
4	6.25		Retrieve Key		
	6.50				Retrieve Key
	6.75		Respond 2		
	7.00				Respond 2
	7.25				
	7.50				
	7.75				
	8.00				

B

Scan	Time	Low Transformation		High Transformation	
		Low Retrieval	High Retrieval	Low Retrieval	High Retrieval
1	0.00				
	0.25	Encode x	Encode x	Encode x	Encode x
	0.50	Encode =	Encode =	Encode -	Encode -
	0.75	Encode a	Encode a	Encode b	Encode b
	1.00	Encode +	Encode +	Encode =	Encode =
	1.25	Encode b	Encode b	Encode a	Encode a
	1.50				
	1.75	Retrieve Key	Retrieve Key	Retrieve -	Retrieve -
2	2.00				
	2.25	Respond +	Respond +	Transform	Transform
	2.50				
	2.75	Encode 4	Encode 7	Retrieve Key	Retrieve Key
	3.00	Encode 0	Encode 3		
	3.25	Encode 8		Respond +	Respond +
	3.50		Retrieve 7-3		
	3.75	Retrieve 4+8		Encode 4	Encode 7
3	4.00		Encode 9	Encode 0	Encode 3
	4.25		Encode 1	Encode 8	
	4.50	Retrieve Key			Retrieve 7-3
	4.75		Retrieve 9-1	Retrieve 4+8	
	5.00	Respond 2			Encode 9
	5.25				Encode 1
	5.50		Retrieve 4+8	Retrieve Key	
	5.75				Retrieve 9-1
	6.00			Respond 2	
4	6.25		Retrieve Key		
	6.50				Retrieve 4+8
	6.75		Respond 2		
	7.00				
	7.25				Retrieve Key
	7.50				
	7.75				Respond 2
	8.00				

Table 3
Parameters estimated and fits to the BOLD response

	Parietal/ Imaginal	Prefrontal/ Retrieval	Parietal/ Retrieval	Prefrontal/ Imaginal
Magnitude (*m*)	3.755	0.995	1.914	1.822
Exponent (*a*)	4.931	4.345	3.179	6.525
Scale (*s*)	1.454	1.168	1.691	1.078
Correlation (*r*)—no-delay	0.974	0.953	0.958	0.917
Correlation (*r*)—delay	0.932	0.898	0.806	0.744
Chi-square—no-delay	99.278	59.326	101.104	118.036
Chi-square—delay	168.548	85.502	394.566	226.927

Fig. 3 for the parietal region and in Fig. 4 for the prefrontal region. The best fitting parameters for the BOLD function in each of these regions are presented in Table 3 along with correlations and Chi-squared statistics to determine the goodness-of-fit of the model predictions to the data. The first two columns in Table 3 are for our predicted mapping of the parietal region onto the imaginal module and the prefrontal region onto the retrieval module. The second two columns present an alternative mapping of the parietal region onto the retrieval module and the prefrontal region onto the imaginal module. The correlations are calculated across all 40 data points for the no-delay condition (4 condition × 10 scan) and across all 56 data points for the no-delay condition (4 condition × 14 scan). For the no-delay condition, the Chi-squared statistics has 37 degrees of freedom, calculated as 40 minus the three parameters estimated for the BOLD function. This results in Chi-squared values greater than 52 representing significant differences ($p < 0.05$). For the delay condition, the Chi-square has 53 degrees of freedom. This results in Chi-squared values greater than 71 representing significant differences ($p < 0.05$).

Although there are some obvious points of disagreement between the model predictions and the data (e.g., the underestimation of the second peak in the delay condition in the parietal region), generally the model fits the qualitative aspects of the data reasonably well. In both regions the model differs significantly from the data, but more so in the delay condition. This suggests that participants were doing something during the delay that we are not accounting for in our model. It is worth noting that in terms of both correlations and Chi-squared deviations, data in each region are better fit by activity in its associated module than the other module. That is, data in the parietal region are fit better by the imaginal module than by the retrieval module, and data in the prefrontal region are fit better by the retrieval module than by the imaginal module. This lends some support to our current mapping of ACT-R modules onto brain regions. The ratio of the probabilities under the two mappings is equal to the exponential of half the Chi-squared differences. Thus, in the no-delay condition the mapping of parietal onto imaginal is 2.5 times more probable than the mapping of the parietal onto the retrieval. In the case of the other 3 mappings, the prescribed mapping is astronomically more probable.

Conclusions

We found that manipulating the retrieval demands and the transformational requirements of algebra problems resulted in differential activity in an overlapping group of regions, including both the prefrontal cortex and the posterior parietal cortex. While the findings of this study were not in accordance with our initial predictions, we were able to better interpret our results with guidance from cognitive modeling. By starting with a model that concurred with our initial predictions and adjusting it so that it fit the response time data, we were able to better understand the plausible effects of our manipulations on the underlying cognitive processes. Changing the model such that it closely matched the response time data actually leads to predictions that were very different from our initial predictions, and concurred with our neuroimaging results. This study underscores the importance of cognitive modeling and demonstrates how it can be utilized to understand the cognitive processes underlying behavioral and neuroimaging data. Specifically, by using cognitive modeling to account for behavioral effect sizes, one can garner a better understanding of the probable cognitive effects of task manipulations. ACT-R turned out to be a powerful architecture with which to accomplish this because it made precise predictions about reaction times and effect sizes, but the same methodology could be applied with any sufficiently precise cognitive model.

With respect to the role of parietal and prefrontal regions in algebra problem solving, our results once again confirm their involvement but also underscore how tightly they are intertwined. While we were better able to fit the BOLD data assuming parietal activation reflected imaginal operations and prefrontal activation reflected retrieval operations, both regions were involved in both the transformation and retrieval stages of the task. We had hoped that the first transformation stage would only manipulate imaginal operations, but our modeling demonstrated that performing such a transformation requires a retrieval from memory. In addition, we had hoped the second retrieval stage would only manipulate retrieval operations but our model suggested that participants optimize their performance by eliminating unnecessary encoding steps. Based on this concerted effort using cognitive modeling and neuroimaging, it seems that it may not be possible to unwind these two processes, at least in a mathematical context. As noted in the introduction the essence of mathematical reasoning involves an interaction between representation and knowledge. It may not be possible to isolate one from the other in any task that maintains its identity as an instance of mathematical reasoning.

Acknowledgments

This work was supported by NIMH award MH068243 to J.R. Anderson. We thank Mark Wheeler, Miriam Rosenberg-Lee, Jennifer Ferris, and an anonymous reviewer for their helpful comments on this manuscript.

Fig. 6. Behavior of the pure manipulation model (A) and mixed manipulation model (B) in the four transformation and retrieval conditions represented in Fig. 1. Imaginal operations are highlighted in light grey and retrieval operations are highlighted in dark grey. The delay condition can be modeled by inserting 8 s of inactivity after the first response.

Appendix A

High and low transformation equations

x-Isolated form	Simplification operation	High transformation	Low transformation
$x=a+b$	$-a$	$x+a=a+b+a$	$x+0=a+b+0$
	$+a$	$x-a=b$	$x=a+b$
	$/a$	$x*a=a*a+a*b$	$1*x=1*a+1*b$
	$*a$	$x/a=1+b/a$	$x/1=a+b/1$
	$-b$	$x+b=a+b+b$	$x+0=a+b+0$
	$+b$	$x-b=a$	$x=a+b$
	$/b$	$x*b=a*b+b*b$	$1*x=1*a+1*b$
	$*b$	$x/b=a/b+1$	$x/1=a+b/1$
$x=a-b$	$-a$	$x+a=a+a-b$	$x+0=a-b+0$
	$+a$	$x-a=0-b$	$x-0=a-b$
	$/a$	$a*x=a*a-a*b$	$1*x=1*a-1*b$
	$*a$	$x/a=1-b/a$	$x/1=a-b/1$
	$-b$	$x+b=a$	$x=a-b$
	$+b$	$x-b=a-b-b$	$x-0=a-b-0$
	$/b$	$b*x=b*a-b*b$	$1*x=1*a-1*b$
	$*b$	$x/b=a/b-1$	$x/1=a-b/1$
$x=a*b$	$-a$	$x+a=a+a*b$	$x+0=a*b+0$
	$+a$	$x-a=a*b-a$	$x-0=a*b-0$
	$/a$	$a*x=a*a*b$	$1*x=1*a*b$
	$*a$	$x/a=b$	$x=a*b$
	$-b$	$x+b=a*b+b$	$x+0=a*b+0$
	$+b$	$x-b=a*b-b$	$x-0=a*b-0$
	$/b$	$b*x=a*b*b$	$1*x=1*a*b$
	$*b$	$x/b=a$	$x=a*b$
$x=a/b$	$-a$	$x+a=a/b+a$	$x+0=a/b+0$
	$+a$	$x-a=a/b-a$	$x-0=a/b-0$
	$/a$	$a*x=a*a/b$	$1*x=1*a/b$
	$*a$	$x/a=1/b$	$x/1=a/b$
	$-b$	$x+b=a/b+b$	$x+0=a/b+0$
	$+b$	$x-b=a/b-b$	$x-0=a/b-0$
	$/b$	$b*x=a$	$x=a/b$
	$*b$	$x/b=a/(b*b)$	$x/1=1/(1*b)$

References

Alivisatos, B., Petrides, M., 1997. Functional activation of the human brain during mental rotation. Neuropsychologia 35, 111–118.

Anderson, J.R., 2005. Human symbol manipulation within an integrated cognitive architecture. Cogn. Sci. 29, 313–341.

Anderson, J.R., in press. Using brain imaging to guide the development of a cognitive architecture. In: Gray, W.D., (Ed.), Integrated Models of Cognitive Systems. New York: Oxford Univ. Press.

Anderson, J.R., Reder, L.M., Lebiere, C., 1996. Working memory: activation limitations on retrieval. Cogn. Psychol. 30, 221–256.

Anderson, J.R., Qin, Y., Sohn, M.-H., Stenger, V.A., Carter, C.S., 2003. An information-processing model of the BOLD response in symbol manipulation tasks. Psychon. Bull. Rev. 10, 241–261.

Anderson, J.R., Bothell, D., Byrne, M.D., Douglass, S., Lebiere, C., Qin, Y., 2004. An integrated theory of the mind. Psychol. Rev. 111, 1036–1060.

Badre, D., Wagner, A.D., 2005. Frontal lobe mechanisms that resolve proactive interference. Cereb. Cortex 15, 2003–2012.

Boyton, G.M., Engel, S.A., Glover, G.H., Heeger, D.J., 1996. Linear systems analysis of functional magnetic resonance imaging in human V1. J. Neurosci. 16, 4207–4221.

Buckner, R.L., Kelley, W.M., Petersen, S.E., 1999. Frontal cortex contributes to human memory formation. Nat. Neurosci. 2, 311–314.

Cabeza, R., Dolcos, F., Graham, R., Nyberg, L., 2002. Similarities and differences in the neural correlates of episodic memory retrieval and working memory. NeuroImage 16, 317–330.

Carpenter, P.A., Just, M.A., Keller, T.A., Eddy, W., Thulborn, K., 1999. Graded function activation in the visuospatial system with the amount of task demand. J. Cogn. Neurosci. 11, 9–24.

Clark, D., Wagner, A.D., 2003. Assembling and encoding word representations: fMRI subsequent memory effects implicate a role for phonological control. Neuropsychologia 41, 304–317.

Cohen, M.S., 1997. Parametric analysis of fMRI data using linear systems methods. NeuroImage 6, 93–103.

Dale, A.M., Buckner, R.L., 1997. Selective averaging of rapidly presented individual trials using fMRI. Hum. Brain Mapp. 5, 329–340.

Davachi, L., Maril, A., Wagner, A.D., 2001. When keeping in mind supports later bringing to mind: neural markers of phonological rehearsal predict subsequent remembering. J. Cogn. Neurosci. 13, 1059–1070.

Dehaene, S., Spelke, E., Pinel, P., Stanescu, R., Tsivkin, S., 1999. Sources of mathematical thinking: behavioral and brain-imaging evidence. Science 284, 970–974.

Dobbins, I.G., Wagner, A.D., 2005. Domain-general and domain-sensitive prefrontal mechanisms for recollecting events and detecting novelty. Cereb. Cortex 15, 1768–1778.

Fletcher, P.C., Henson, R.N.A., 2001. Frontal lobes and human memory: insights from functional neuroimaging. Brain 124, 849–881.

Fletcher, P.C., Frith, C.D., Baker, S.C., Shallice, T., Frackowiak, S.J., Dolan, R.J., 1995. The mind's eye — precuneus activation in memory-related imagery. NeuroImage 2, 195–200.

Glover, G.H., 1999. Deconvolution of impulse response in event-related BOLD fMRI. NeuroImage 9, 416–429.

Heil, M., 2002. Early career award: the functional significance of ERP effects during mental rotation. Psychophysiology 39, 535–545.

Köhler, S., Paus, T., Buckner, R.L., Milner, B., 2004. Effects of left inferior prefrontal stimulation on episodic memory formation: two-stage fMRI-rTMS study. J. Cogn. Neurosci. 16, 178–188.

Lepage, M., Ghaffar, O., Nyberg, L., Tulving, E., 2000. Prefrontal cortex and episodic memory retrieval mode. Proc. Natl. Acad. Sci. U. S. A. 97, 506–511.

National Council of Teachers of Mathematics, 2000. Principles and Standards for School Mathematics. NCTM, Reston, VA.

Qin, Y., Sohn, M.-H., Anderson, J.R., Stenger, V.A., Fissell, K., Goode, A., Carter, C.S., 2003. Predicting the practice effects on the blood oxygenation level-dependent (BOLD) function of fMRI in a symbolic manipulation task. Proc. Natl. Acad. Sci. 100, 4951–4956.

Qin, Y., Carter, C.S., Silk, E.M., Stenger, A., Fissell, K., Goode, A., Anderson, J.R., 2004. The change of brain activation patterns as children learn algebra equation solving. Proc. Natl. Acad. Sci. 101, 5686–5691.

Reichle, E.D., Carpenter, P.A., Just, M.A., 2000. The neural basis of strategy and skill in sentence–picture verification. Cogn. Psychol. 40, 261–295.

Richter, W., Ugurbil, K., Georgopoulos, A., Kim, S.-G., 1997. Time-resolved fMRI of mental rotation. NeuroReport 8, 3697–3702.

Rossi, S., Cappa, S.F., Babiloni, C., Pasqualetti, P., Miniussi, C., Carducci, F., Babiloni, F., Rossini, P.M., 2001. Prefrontal cortex in long-term memory: an "interference" approach using magnetic stimulation. Nat. Neurosci. 4, 948–952.

Rossi, S., Pasqualetti, P., Zito, G., Vecchio, F., Cappa, S.F., Miniussi, C., Babiloni, C., Rossini, P.M., 2006. Prefrontal and parietal cortex in human episodic memory: an interference study by repetitive transcranial magnetic stimulation. Eur. J. Neurosci. 23, 793–800.

Rugg, M.D., Henson, R.N.A., 2002. Episodic memory retrieval: an (event-related) functional neuroimaging perspective. In: Parker, A., Wilding, E., Bussey, T. (Eds.), The Cognitive Neuroscience of Memory: Encoding and Retrieval. Psychocology Press, Hove, pp. 3–37.

Sohn, M.-H., Goode, A., Stenger, V.A., Carter, C.S., Anderson, J.R., 2003. Competition and representation during memory retrieval: roles of prefrontal cortex and posterior parietal cortex. Proc. Natl. Acad. Sci. 100, 7412–7417.

Sohn, M.-H., Goode, A., Koedinger, K.R., Stenger, V.A., Fissell, K., Carter, C.S., Anderson, J.R., 2004. Behavioral equivalence, but not neural equivalence — neural evidence of alternative strategies in mathematical thinking. Nat. Neurosci. 7, 1193–1194.

Sohn, M.-H., Goode, A., Stenger, V.A., Carter, C.S., Anderson, J.R., 2005. An information-processing model of three cortical regions: evidence in episodic memory retrieval. NeuroImage 25, 21–33.

Stuss, D.T., Benson, D.F., 1984. Neuropsychological studies of the frontal lobes. Psychol. Bull. 95, 3–28.

Shimamura, A.P., 2005. Memory and frontal lobe function. In: Gazzaniga, M.S. (Ed.), The Cognitive Neurosciences. MIT Press, Cambridge, MA, pp. 803–813.

Thompson-Schill, S.L., 2003. NeuroImaging studies of semantic memory: inferring "how" from "where". Neuropsychologia 41, 280–292.

Wagner, A.D., Maril, A., Bjork, R.A., Schacter, D.L., 2001a. Prefrontal contributions to executive control: fMRI evidence for functional distinctions within lateral prefrontal cortex. NeuroImage 14, 1337–1347.

Wagner, A.D., Paré-Blagoev, E.J., Clark, J., Poldrack, R.A., 2001b. Recovering meaning: left prefrontal cortex guides controlled semantic retrieval. Neuron 31, 329–338.

Wagner, A.D., Shannon, B.J., Kahn, I., Buckner, R.L., 2005. Parietal lobe contributions to episodic memory retrieval. Trends Cogn. Sci. 9, 445–453.

Woods, R.P., Grafton, S.T., Holmes, C.J., Cherry, S.R., Mazziotta, J.C., 1998. Automated image registration: I. General methods of intrasubject, intramodality variation. J. Comput. Assist. Tomogr. 22, 139–152.

Zacks, J.M., Ollinger, J.M., Sheridan, M.A., Tversky, B., 2002. A parametric study of mental spatial transformation of bodies. NeuroImage 16, 857–872.